HHS Public Access

Author manuscript

Cleft Palate Craniofac J. Author manuscript; available in PMC 2022 May 01.

Published in final edited form as:

Cleft Palate Craniofac J. 2022 May ; 59(5): 614–621. doi:10.1177/10556656211014070.

A Preliminary Study of Anatomical Changes Following the Use of a Pedicled Buccal Fat Pad Flap During Primary Palatoplasty

Katelyn J Kotlarek[1], **Michael S Jaskolka**[2], **Xiangming Fang**[3], **Charles Ellis**[4], **Silvia S Blemker**[5], **Bruce Horswell**[6], **Paul Kloostra**[7], **Jamie L Perry**[4]

[1]Division of Communication Disorders, University of Wyoming, Laramie, WY, USA.

[2]New Hanover Regional Medical Center, Wilmington, NC, USA.

[3]Department of Biostatistics, East Carolina University, Greenville, NC, USA.

[4]Department of Communication Sciences and Disorders, East Carolina University, Greenville, NC, USA.

[5]Department of Biomedical Engineering, University of Virginia, Charlottesville, VA, USA.

[6]Indiana University Hospital, Indianapolis, IN, USA.

[7]Charleston Area Medical Center, Charleston, WV, USA.

Abstract

Objective: The purpose of this study was to examine the surgical impact of the pedicled BFP flap on the LVP muscle and surrounding VP anatomy following primary palatoplasty.

Design: Observational, prospective

Setting: MRI studies were completed at 3 imaging facilities. All participants with BFP flap were operated on by the same surgeon.

Participants: Five pediatric participants with CP±L who underwent primary palatoplasty with BFP flap placement. Comparison groups consisted of 10 participants: 5 with CP±L who did not receive the BFP flap and 5 healthy controls.

Interventions: All participants underwent nonsedated MRI 2–5 years postoperatively.

Main Outcomes and Measures: Anatomical measures of the velopharynx and LVP among the 3 participant groups

Results: Median values were significantly different among groups for velar length ($p = .042$), effective velar length ($p = .048$), effective VP ratio ($p = .046$), LVP length ($p = .021$), extravelar LVP length ($p = .009$), and LVP origin-origin distance ($p = .030$). Post hoc analysis revealed a statistically significant difference between the BFP and traditional repair groups for effective VP ratio ($p = .040$), extravelar LVP length ($p = .033$), and LVP length ($p = .022$).

Corresponding Author: Katelyn J. Kotlarek, Division of Communication Disorders, 1000 E. University Ave, Dept 3311, Health Sciences, 253, Laramie, WY 82071, USA. kkotlare@uwyo.edu.

Conclusions: This study provides preliminary support that the BFP flap creates a longer velum, with increased distance between the posterior hard palate and the LVP, and a larger effective VP ratio compared to traditional surgical techniques. Future research is needed to determine if this procedure provides a more favorable mechanism for VP closure.

Keywords

palatoplasty; outcomes; MRI

Introduction

Children born with a cleft palate with or without cleft lip (CP±L) typically undergo primary palatoplasty during infancy. Currently, there are various surgical techniques used during primary palatoplasty, which differ between centers and among surgeons (Agrawal, 2009). Current literature suggests that positive outcomes are apparent 70–80% of the time regardless of the type of procedure used (Musgrave and Bremner, 1960; Moore, et al., 1988; Marsh et al., 1989; Phua and de Chalain, 2008; Sullivan, et al., 2009). It is estimated that 9–37% of these children require additional surgical management to address velopharyngeal insufficiency (VPI; Bicknell et al., 2002; Lithovius et al., 2014; Timbang et al., 2014; Sitzman et al., 2019).

The BFP flap (or graft) has been utilized with numerous surgical modifications during primary palatoplasty (Kim, 2001; Pinto and Debnath, 2007; Pappachan and Vasant, 2008; Levi et al., 2009; Zhang, et al. 2010; Grobe et al., 2011; Zhang, et al. 2015; Yamaguchi et al., 2016; Adevamo et al., 2019; Horswell and Chou, 2019; Qiu et al., 2019; Kim et al., 2020). Of these studies, half positioned a pedicled BFP flap at the junction of the hard and soft palate (Pinto and Debnath, 2007; Zhang et al., 2010; Grobe et al., 2011; Horswell and Chou, 2019; Qiu et al., 2019; Kim et al., 2020). Necrosis of the pedicled BFP flap and postoperative perforation are said to not occur if care is taken to avoid lacerating the capsule of the BFP (Zhang et al., 2010). It has been hypothesized that the pedicled BFP flap, when placed along the posterior border of the hard palate, results in an increase in vascularized tissue within the palate, preventing wound contracture and reducing superficial dehiscence of the oral mucosa (Zhang et al., 2010; Qiu et al., 2019). Others further propose that the use of a pedicled BFP flap creates a longer velum while not inhibiting maxillary growth (Zhang et al., 2010; Grobe et al., 2011). Noted advantages of using the BFP flap over other surgical techniques that add tissue to the palate, such as the buccal myomucosal flap or tongue flap, include the lack of a secondary surgical site, reduced chances of injuring the Stenson duct, and quick epithelialization due to the abundant blood supply (Levi et al., 2009; Zhang et al., 2010; Grobe et al., 2011). However, these hypotheses have not been systematically examined and compared to children with cleft palate not receiving a BFP flap nor children without cleft palate. Outcome studies to date have been restricted to retrospective analyses based on patients receiving varied BFP flap surgical techniques, including location and use of the BFP flap as well as palatal closure techniques.

The purpose of this study was to examine the surgical impact of the pedicled BFP flap on the levator veli palatini (LVP) muscle and surrounding velopharyngeal (VP) anatomy

following primary palatoplasty. It was hypothesized that participants with cleft palate treated with the pedicled BFP flap would exhibit VP dimensions more similar to those of non-cleft participants. Additionally, a longer, thicker velum and more favorable VP ratio were anticipated in the BFP group when compared to participants with cleft palate treated with traditional repair techniques.

Methods

Data Collection

Fifteen English-speaking children aged 3–7 years participated in this study, which was approved by all associated Intuitional Review Boards. Since previous research has shown sex effects to be nonsignificant within this age range, this variable was not controlled for in recruitment (Perry et al., 2018). Participants were prospectively recruited and enrolled consecutively as part of three study groups. Ten of the participants had a history of repaired CP±L, half of which received a pedicled BFP flap during primary palatoplasty and the other half received a traditional repair without the addition of any tissue. Five participants with non-cleft anatomy were prospectively recruited for normative comparison. None of the participants had received any form of secondary palate repair at the time of the MRI study. All participants in this study presented with typical resonance and no perceptual signs of VPI, as determined through perceptual resonance evaluation at the time of the MRI study by a speech-language pathologist with experience in craniofacial speech evaluations. Resonance classification was further supported by documentation obtained in the most recent craniofacial team report.

Primary palatoplasty was completed prior to initiation of this study (between 6–18 months of age) and used to determine group inclusion. Timing of palatoplasty and procedure type were confirmed through surgical operative notes. During surgery, all repairs involving pedicled BFP flap placement at the palatine aponeurosis were completed by the same craniofacial surgeon (MSJ). Within the BFP flap group, one participant received a double-opposing Z-plasty while the other 4 received an intravelar veloplasty. In both cases, underlying dissection of the muscle tissue from the back of the hard palate and division of the tensor tendon was completed. The nasal layer of the soft and hard palate was closed, and the remainder of the uvula was reconstructed. In the participant who received a double-opposing Z-plasty procedure, the remainder of soft palate reconstruction was completed prior to the dissection of the pedicled BFP flap. In the participants who underwent intravelar veloplasty, the muscle dissection and reconstruction was completed prior to the dissection of the pedicled BFP flap. The posterior portion of the lateral releasing incisions were used to access the buccal vestibule. Submucosal blunt dissection was used to identify the BFP, which was teased into the space of Ernst and then brought through a tension-free tunnel underneath the oral flap posteriorly to the neurovascular bundle. If a unilateral BFP flap was employed, it was sutured to the contralateral posterior edge of the hard palate; bilateral BFP flaps were sutured together in the midline. Of note, the single participant who received the bilateral BFP flaps underwent an intravelar veloplasty. The oral side was closed at midline and several horizontal mattress sutures were placed at the junction of the hard and soft

palate. The remainder of the oral side was closed without tension. Repairs among those without a BFP flap were completed by different surgeons with varying surgical technique.

The MRI protocol, processing, and analysis were consistent with previous investigations of the velopharynx. This study implemented the use of a non-sedated, child-friendly protocol previously published by Kollara and Perry (2014). On the day of the MRI study, written consent was obtained from the participant's legal guardian, and written assent was obtained from the participant if they were of age per Institutional Review Board requirements. Participants were provided with ear plugs and headphones, and their head was secured with towels and cushions to fit snugly in the head coil. Three MRI scanners (2, 1.5 Tesla and 1, 3 Tesla Siemens) were used to implement this study due to geographical distance within the recruitment area. Reliability has previously been established between 1.5 Tesla and 3 Tesla magnets for MRI of the velopharyx (Perry et al., 2018). Participants were not sedated. Children were imaged using a high resolution, T2-weighted turbo-spin-echo three-dimensional anatomical scan (SPACE) to acquire a large field of view covering the oropharyngeal anatomy with a minimum of 0.8 mm isotropic resolution and an acquisition time of less than 5 minutes. Head rotation was minimized by use of cushions around the head. These imaging sequences described previously (Bae et al., 2011; Perry et al., 2013) provided a data set of the structures of interest. Image processing was completed using Thermo Scientific™ Amira™ Software (Thermo Fisher Scientific, Waltham, MA, US). This program has a native Digital Imaging and Communication in Medicine (DICOM) support program which preserves the original anatomical geometry. Points of interest for measures of the velopharynx can be visualized in Figure 1. Points of interest for measures of the LVP muscle can be visualized in Figure 2. Variable definitions are consistent with those cited by Kotlarek and colleagues (2020).

Statistical Analysis

Due to the small sample size and non-normal distribution of data, nonparametric statistical analyses were utilized for comparing measures between the aforementioned participant groups: "non-cleft" (n=5), "traditional cleft" (n=5), and "cleft with BFP" (n=5). All assumptions were adequately met for the Kruskal-Wallis H test. Pairwise comparisons were conducted when applicable using a Bonferroni correction for multiple comparisons, and adjusted *p*-values were presented. Median values are presented due to outliers in the data.

Using an intra-class correlation, reliability was completed on 80% of participants 4 weeks after initial data analysis. An intra-class correlation ($\alpha = .05$) was used to assess inter- and intra-rater reliability. Reliability was completed on 80% of participants using one linear and one angle measure due to angles having the lowest reliability in previously reported MRI studies of the VP mechanism. Inter-rater reliability was r = .813 for effective velar length and r = .762 for sagittal angle, which was calculated using separate measurements competed by two researchers with a minimum of 4 years' experience in 3D MRI data analyses. Intra-rater reliability was completed on the same set of linear and angle measures 4 weeks later. Intra-rater reliability was r = .951 and .995, respectively, for these selected measures. Observed differences in intra- versus inter-rater reliability were likely due to image selection

prior to measuring. Regardless, reliability of all measures showed good (r = .75–.90) to excellent agreement (r = .90+; Portney and Watkins, 2000).

Results

Multiple Kruskal–Wallis H tests were utilized to determine if there were differences in the variables among the three groups of participants. Due to the nature of these nonparametric statistical methods and the small sample size, the influence of growth was not considered in further analysis. Additionally, participant age was not significantly different ($\chi^2(2) = 2.580$, $p = .275$) among the non-cleft (M = 6.26 years, Mdn = 6.66 years), traditional cleft (M = 6.02 years, Mdn = 5.54 years), and cleft with BFP (M = 4.57 years, Mdn = 3.67 years) groups. Participants in the normative and BFP groups were all Caucasian. Participants in the traditional cleft group contained three participants who were Caucasian (one Hispanic), one Asian, and one African American. Although race has been shown to be significantly different among groups in children (Perry et al., 2018), it was not considered as a variable within this study because the limited sample size would not allow for adequate statistical comparison.

Regarding measures of the velopharynx, median values were significantly different across groups for velar length, $\chi^2(2) = 6.320$, $p = .042$. Median velar length measures increased from traditional cleft (19.10 mm) to non-cleft (27.70 mm) to cleft with BFP (28.60 mm) groups. Post hoc analysis revealed a significant difference in velar length between the non-cleft (mean rank = 10.80) and traditional cleft (mean rank= 4.00; $p = .049$) groups but not between any other group combination. Median values were also significantly different for effective velar length, $\chi^2(2) = 6.080$, $p = .048$, increasing from traditional cleft (11.51 mm) to non-cleft (11.82 mm) to cleft with BFP (17.37 mm) groups. Post hoc analysis revealed no significant pairwise comparisons for effective velar length; however, the differences between the traditional cleft (mean rank = 6.60) and cleft with BFP (mean rank = 12.00, $p = .071$) groups were approaching significance. Median values were significantly different for effective VP ratio, $\chi^2(2) = 6.140$, $p = .046$, increasing from traditional cleft (0.61) to non-cleft (0.70) to cleft with BFP (1.20) groups. Post hoc analysis revealed a statistically significant difference in effective VP ratio between the traditional cleft (mean rank = 4.60) and cleft with BFP (mean rank = 11.60, $p = .040$) groups but not between any other group combination. Remaining measures of the velopharynx were not found to be significantly different among groups. Results regarding VP dimensions are depicted in Table 1.

With respect to the LVP, median values were significantly different for LVP origin-to-origin distance, $\chi^2(2) = 7.020$, $p = .030$, increasing from cleft with BFP (44.67 mm) to traditional cleft (49.70 mm) to non-cleft (55.15 mm) groups. Post hoc analysis revealed a statistically significant difference in LVP origin-to-origin distance between the cleft with BFP (mean rank = 3.80) and non-cleft (mean rank = 11.00; $p = .033$) groups but not between any other group combination. Median values were also significantly different for LVP length, $\chi^2(2) = 7.760$, $p = .021$, increasing from cleft with BFP (33.48 mm) to non-cleft (36.73 mm) to traditional cleft (38.89 mm) groups. Post hoc analysis revealed a statistically significant difference in LVP length between the traditional cleft (mean rank = 11.20) and cleft with BFP (mean rank = 3.60, $p = .022$) groups but not between any other group combination.

Median values were significantly different for extravelar length, $\chi^2(2) = 9.420$, $p = .009$. Median extravelar length increased from cleft with BFP (23.28 mm) to traditional cleft (25.64 mm) to non-cleft (26.55 mm) groups. Post hoc analysis revealed a statistically significant difference in extravelar length between the cleft with BFP (mean rank = 3.00) and non-cleft (mean rank = 10.80; $p = .033$) groups as well as between the cleft with BFP (mean rank = 3.00) and traditional cleft (mean rank = 10.20; $p = .017$) groups. Remaining measures of the LVP muscle were not found to be significantly different among groups. Results regarding LVP muscle dimensions are depicted in Table 2.

Discussion

This study utilized non-sedated MRI to examine the surgical impact of the pedicled BFP flap on LVP and surrounding VP anatomy following primary palatoplasty. Significant differences among the three groups were observed for velar length, effective velar length, effective VP ratio, LVP origin-to-origin distance, LVP length, and extravelar LVP length.

When the LVP sling is restored at the velar midline during primary palatoplasty, there is likely an area of submucosal dead space covered by oral and nasal mucosa at the posterior hard palate. It has been hypothesized that this denude region causes the surgically retropositioned LVP sling to migrate anteriorly to its original position (Zhang et al., 2010). It is also possible this anterior migration may tether the palate anteriorly as the oral and nasal mucosa scar together with minimal submucosal tissue, resulting in limited velar stretch and a more anteriorly positioned LVP sling. Rather, the BFP might serve as a buffer to prevent anterior LVP muscle migration, and the addition of adipose tissue may actually create a more supple and thicker palate. While the BFP flap was visualized via MRI (Kotlarek et al., *under review*), its location did not result in a change in velar thickness as expected.

Midsagittal images of all participants in the cleft with BFP group can be visualized in Figure 3, showing the pedicled BFP flap present as a light gray mass at the junction between the hard and soft palate. This finding offers quantitative support that the BFP flap is maintained to some degree within the palate and may act as a space holder to prevent the LVP muscle fibers from moving anteriorly while increasing the distance between the posterior hard palate and the LVP muscle (effective velar length). The location of the BFP flap at the posterior palate and anterior to the LVP sling inherently increases effective velar length in these participants. In this study, median effective velar length was longer in the cleft with BFP group than either the non-cleft or traditional cleft groups. The increase in effective velar length resulted in a significant difference observed among the three groups with respect to total velar length as well. Anterior positioning of the LVP has been reported as a key feature related to VPI and an indicator for palate revision (Boorman & Sommerlad, 1985; Sommerlad et al., 1994; Sommerlad et al., 2002). Additionally, reduced effective velar length has been reported in children with repaired cleft palate and VPI (Tian et al. 2010; Kotlarek et al., 2020).

The BFP group had a significantly larger effective VP ratio than the traditional cleft group, which is likely due to the longer effective velar length. In the present study, median values were significantly different for effective VP ratio between traditional cleft and cleft with

BFP groups despite normal resonance observed across all participants. Effective VP ratio is defined as effective velar length divided by pharyngeal depth. A shorter palate and deeper pharynx have been commonly associated with VPI across the literature, and those with repaired cleft palate are prone to having a shorter, thinner velum postoperatively (D'Antonio et al., 2000; Randall et al., 2000). It is possible that an even longer effective velar length than that of non-cleft anatomy may be necessary to maintain comparable LVP positioning. In the present study, those with BFP did demonstrate a longer effective velar length than in the normative group.

As the LVP muscle sling is positioned more posteriorly within the body of the velum, it is expected that the LVP muscle length would decrease because the insertion of the muscle (midline) is closer to the origin (base of the skull). The LVP muscle sling of participants in the cleft with BFP group can be visualized in Figure 3. The cleft with BFP group exhibited a significantly shorter LVP length than the traditional cleft group. The extravelar LVP length in the cleft with BFP group was significantly shorter than both the traditional cleft and non-cleft groups. Compared to their non-cleft counterparts, children with repaired CP±L have been shown to have differences in LVP insertion width and thickness at midline, and specifically those with VPI have a shorter extravelar length. Additionally, adults with repaired cleft palate have been shown to exhibit decreased length, intravelar length, thickness, volume, circumference, diameter, and angles of origin of the LVP (Ha et al., 2007; Kotlarek et al., 2017; Perry et al., 2018). In the present study, a portion of the tensor tendon was cut to release the LVP muscle bundles and push them posteriorly in participants in the cleft with BFP group; all participants in this group also received varying degrees of LVP muscle bundle overlap, which was based on intraoperative assessment of tension in each specific participant. It is unclear how surgical techniques impact the intravelar and extravelar portions of the LVP, and whether or not this is of clinical significance has yet to be determined. Future research is needed to describe the anatomical impact of various surgical approaches on the LVP, including differences between more traditional techniques such as the intravelar veloplasty and double-opposing Z-plasty.

Limitations

This preliminary study has several limitations impacting the extent to which conclusions can be drawn and generalized to population with cleft palate at large. First, this study consisted of a small sample of children. The nonparametric statistical methods employed in this study did not allow for comparison of age, race, cleft type, or surgical procedure type. Although age was not significantly different between groups, the BFP group was younger; however, this group actually displayed measures that showed greater values than the older children for most measures (e.g., velar thickness, velar length). Therefore, differences may become even more apparent if age were used as a covariate in future parametric comparison.

Surgical procedure and/or growth is likely responsible for a portion of the observed differences in muscle morphology and VP status across the literature (Law and Fulton, 1959; McGowan et al., 1992; Ishikawa et al., 1998; Khanna et al., 2012). Although participants with the BFP flap were recruited from a single surgeon's clinical population, the soft palate closure technique varied between participants. In addition, the BFP procedure was

not identical between participants, as a single participant had bilateral BFP flaps placed during primary palatoplasty while the other 4 participants within the BFP group received a unilateral flap.

The present study was limited to participants with normal resonance to isolate the anatomical impact of the pedicled BFP flap on VP anatomy. Significant differences were evident even in the presence of normal resonance, further supporting previous research in children and adults that wide anatomic variability can occur in the presence of typical speech (Ha et al., 2007, Tian et al., 2010; Perry et al., 2018; Kotlarek et al., 2020). Because this study did not include children with VPI, we cannot examine which anatomic variations are of greatest clinical significance and how pre-surgical anatomy impacts VP function for speech. This study represents the first step to understanding the impact of BFP on VP anatomy and supports continued research related to function (e.g., speech). Future studies employing a cohort of participants with VPI while controlling for surgical repair procedure will be imperative to answering this question. Additionally, research employing dynamic MRI methods or computational modeling may provide insight into potential functional changes to velopharyngeal mechanism resulting from the placement of a pedicled BFP flap.

Conclusions

The current study provides insight into the postsurgical anatomy of participants who underwent pedicled BFP flap placement during primary palatoplasty. Results suggest that this surgical technique creates a longer velum, with increased distance between the posterior hard palate and the LVP, and a larger effective VP ratio compared to traditional surgical techniques that do not add tissue to the velum. Additional research employing a larger sample size should be completed to evaluate cases with VPI as well as cross-sectional data across the lifespan to determine if this technique yields improved speech and facial growth outcomes.

References

Adeyemo WL, Ibikunle AA, James O, Taiwo OA. Buccal fat pad: A useful adjunct flap in cleft palate repair. J Maxillofac Oral Surg. 2019;18(1):40–45. [PubMed: 30728690]

Agrawal K Cleft palate repair and variations. Ind J Plast Surg. 2009;42 Suppl:S102–109.

Bae Y, Kuehn DP, Sutton BP, Conway CA, Perry JL. Three-dimensional magnetic resonance imaging of velopharyngeal structures. J Speech Hear Res. 2011;54:1538–1545.

Bicknell S, McFadden LR, Curran JB. Frequency of pharyngoplasty after primary repair of cleft palate. J Can Dent Assoc. 2009;68(11):688–692

Boorman JG, Sommerlad BC. Levator palati and palatal dimples: their anatomy, relationship and clinical significance. Br J Plast Surg1985;38:326–332.

D'Antonio LL, Muntz HR, Province MA, Marsh JL. Laryngeal/voice findings in patients with velopharyngeal dysfunction. Laryngoscope. 1988;98(4):432–438. [PubMed: 3352445]

Grobe A, Eichhorn W, Hanken H, Precht C, Schmelzle R, Heiland M, Blessman M. The use of buccal fat pad (BFP) as a pedicled graft in cleft palate surgery. Int J Oral Maxillofac Surg. 2011;40:685–689 [PubMed: 21470824]

Ha S, Kuehn DP, Cohen M, Alperin N. Magnetic resonance imaging of the levator veli palatini muscle in speakers with repaired cleft palate. Cleft Palate Craniofac J. 2007;44:494–501. [PubMed: 17760495]

Horswell BB, Chou J. Does the CHOP modification improve fistula rate in Furlow double-opposing a-plasty? [Published online September 24, 2019]. J Oral Maxiollofac Surg. 2019. doi: 10.1016/j.joms.2019.08.018

Huang MH, Lee ST, Rajendra KA. A fresh cadaveric study of the paratubal muscles: Implications for eustachian tube function in cleft palate. Plast Reconstr Surg. 1997;100,833–842. [PubMed: 9290650]

Ishikawa H, Nakamura S, Misaki K, Kudoh M, Fukuda H, Yoshida S. Scar tissue distribution on palates and its relation to maxillary dental arch form. Cleft Palate Craniofac J. 1998;35:313–319. [PubMed: 9684769]

Khanna R, Tikku T, Wadhwa J. Nasomaxillary complex in size, position and orientation in surgically treated and untreated individuals with cleft lip and palate: a cephalometric overview. Indian J Plast Surg. 2012;45:68–75. [PubMed: 22754157]

Kim Y The use of a pedicled buccal fat pad graft for bone coverage in primary palatorrhaphy: A case report. Int J Oral Maxillofac Surg. 2001;59:1499–1501.

Kim J, Kim S, Park Y, Hwang DS, Paeng J, Seok H. The effect of buccal fat pad graft int eh palatoplasty and the risk factor of postoperative palatal fistula. J Craniofac Surg. 2020;31(3);658–661. [PubMed: 31985598]

Kollara L, Perry J. Effects of gravity on the velopharyngeal structures in children using upright magnetic resonance imaging. Cleft Palate Craniofac J. 2014;51(6):669–676. [PubMed: 24060001]

Kotlarek KJ, Perry JP, Fang X. Morphology of the levator veli palatini muscle in adults with repaired cleft palate. J Craniofac Surg. 2017;28:833–837. [PubMed: 28060090]

Kotlarek KJ, Perry JL, Jaskolka MS. What is the fate of the pedicled buccal fat pad graft when used during primary palatoplasty? Under review.

Kotlarek KJ, Pelland C, Blemker SS, Jaskolka M, Fang X, Perry JL. Asymmetry and positioning of the levator veli palatini muscle in children with repaired cleft palate. J Speech Lang Hear Res. 2020;63:1317–1325. [PubMed: 32402223]

Law FE, Fulton JT. Unoperated oral clefts at maturation. Am J Public Health. 1959;49:1517–1524.

Levi B, Kasten S, Buchman S. Utilization of the buccal fat pad flap for congenital cleft palate repair. Plast Reconstr Surg. 2009;123(3):1018–1021. [PubMed: 19319069]

Lithovius RH, Ylikontiola LP, Sandor GK. Frequency of pharyngoplasty after primary repair of cleft palate in northern Finland. Oral Surg, Oral Med, Oral Path, Oral Rad. 2014;117(4):430–434.

Marsh JL, Grames LM, Holtman, Intravelar veloplasty: A prospective study. Cleft Palate J. 1989;26(1):6–50.

McGowan JC, Hatabu H, Yousem DM, Randall P, Kressel HY. Evaluation of soft palate function with MRI: Application to the cleft palate patient. J Comput Assist Tomogr. 1992;16:877–882. [PubMed: 1430434]

Moore MD, Lawrence WT, Ptak JJ, Trier WC. Complications of primary palatoplasty: A twenty-one-year review. Cleft Palate J. 1988;25(2):156–162. [PubMed: 3163291]

Musgrave RH, Bremner JC. Complications of cleft palate surgery. Plas Reconstr Surg. 1960;26(2):180.

Pappachan B, Vasant R. Application of bilateral pedicled buccal fat pad in wide primary cleft palate. Brit J Oral Maxillofac Surg. 2008;46,310–312. [PubMed: 17640783]

Perry JL, Kuehn DP, Sutton BP. Morphology of the levator veli palatini muscle using magnetic resonance imaging. Cleft Palate Craniofac J. 2013;50:64–75. [PubMed: 22023112]

Perry JL, Kollara L, Kuehn DP, Sutton BP, Fang X. Examining age, sex, and race characteristics of velopharyngeal structures in 4- to 9- year old children using magnetic resonance imaging. Cleft Palate Craniofac J. 2018;55(1):21–34. [PubMed: 33948051]

Perry JL, Kotlarek KJ, Sutton BP, Kuehn DP, Jaskolka MS, Fang X, Point SW, Rauccio F. Variations of velopharyngeal structure in adults with repaired cleft palate. Cleft Palate Craniofac J. 2018;55(10):1409–1418. [PubMed: 29356620]

Pigott R An analysis of the strengths and weaknesses of endoscopic and radiological investigations of velopharyngeal incompetence based on a 20 year experience of simultaneous recording. Br J Plast Surg. 2002;55(1):32–34. [PubMed: 11783966]

Pinto P, Debnath S. Use of pedicled graft of buccal fat pad to line a nasal defect in releasing pushback palatoplasty. Brit J Oral Maxillofac Surg. 2007;45:249–250. [PubMed: 17064829]

Phua YS, de Chalain T. Incidence of oronasal fistulae and velopharyngeal insufficiency after cleft palate repair: An audit of 211 children born between 1990 and 2004. Cleft Palate Craniofac J. 2008;45(2):172–178. [PubMed: 18333650]

Portney LG, Watkins MP. Foundations of Clinical Research: Application to Practice. Upper Saddle River, NJ: Prentice Hall; 2000.

Qui CS, Fracol ME, Bae H, Gosain AK. Prophylactic use of buccal fat flaps to improve oral mucosal healing following Furlow palatoplasty. Plast Reconstr Surg. 2019;143:1179–1183. [PubMed: 30921142]

Randall R, LaRossa D. McWilliams B, Cohen M, Solot C, Jawad A. Palate length as a predictor of speech outcome. Plast Reconstr Surg 2000;106:1254–1259. [PubMed: 11083554]

Sitzman TJ, Carle AC, Heaton PC, Helmrath MA, Britto MT. Five-fold variation among surgeons and hospitals in the use of secondary palate surgery. Cleft Palate Craniofac J. 2019;56(5):586–594. [PubMed: 30244603]

Sommerlad BC, Henley M, Birch M, Harland K, Moiemen N, Boorman JG. Cleft palate re-repair-a clinical and radiographic study of 32 consecutive cases. Br J Plast Surg. 1994;47:406–410. [PubMed: 7952806]

Sommerlad BC, Mehendale FV, Birch MJ, Sell D, Hattee C, Harland K. Palate re-repair revisited. Cleft Palate Craniofac J. 2002;39(3):295–307. [PubMed: 12019005]

Sullivan SR, Marrinan EM, LaBrie RA, Rogers GF, Mulliken JB. Palatoplasty outcomes in nonsyndromic patients with cleft palate: A 29-year assessment of one surgeon's experience. J Craniofac Surg. 2009;20:612–616. [PubMed: 19169156]

Tian W, Yin H, Li Y, Zhao S, Zheng Q, Shi B. Magnetic resonance imaging of velopharyngeal structures in Chinese children after primary palatal repair. J Craniofac Surg. 2010;21:568–577. [PubMed: 20216435]

Timbang MR, Gharb BB, Rampazzo A, Papay F, Zins J, Doumit G. A systematic review comparing Furlow double-opposing z-platy and straight-line intravelar veloplasty methods of cleft palate repair. Plast Reconstr Surg. 2014;134(5):1014–1022. [PubMed: 25347635]

Yamaguchi K, Lonic D, Lee C, Yun C, Lo L, Modified Furlow palatoplasty using small double-opposing Z-plasty: Surgical technique and outcome. Plast Reconstr Surg. 2016;137(6):1825–1831. [PubMed: 27219237]

Zhang Q, Li L, Tan W, Chen L, Gao N, Bao, C. Application of unilateral pedicled buccal fat pad for nasal membrane closure in the bilateral complete cleft palate. J Oral Maxillofac Surg. 2010;68:2029–2032. [PubMed: 20542618]

Zhang M, Zhang X, Zheng C. Application of buccal fat pads in pack palate relaxing incisions on maxillary growth: A clinical study. Int J Clin Exp Med. 2015;8(2):2689–2692. [PubMed: 25932221]

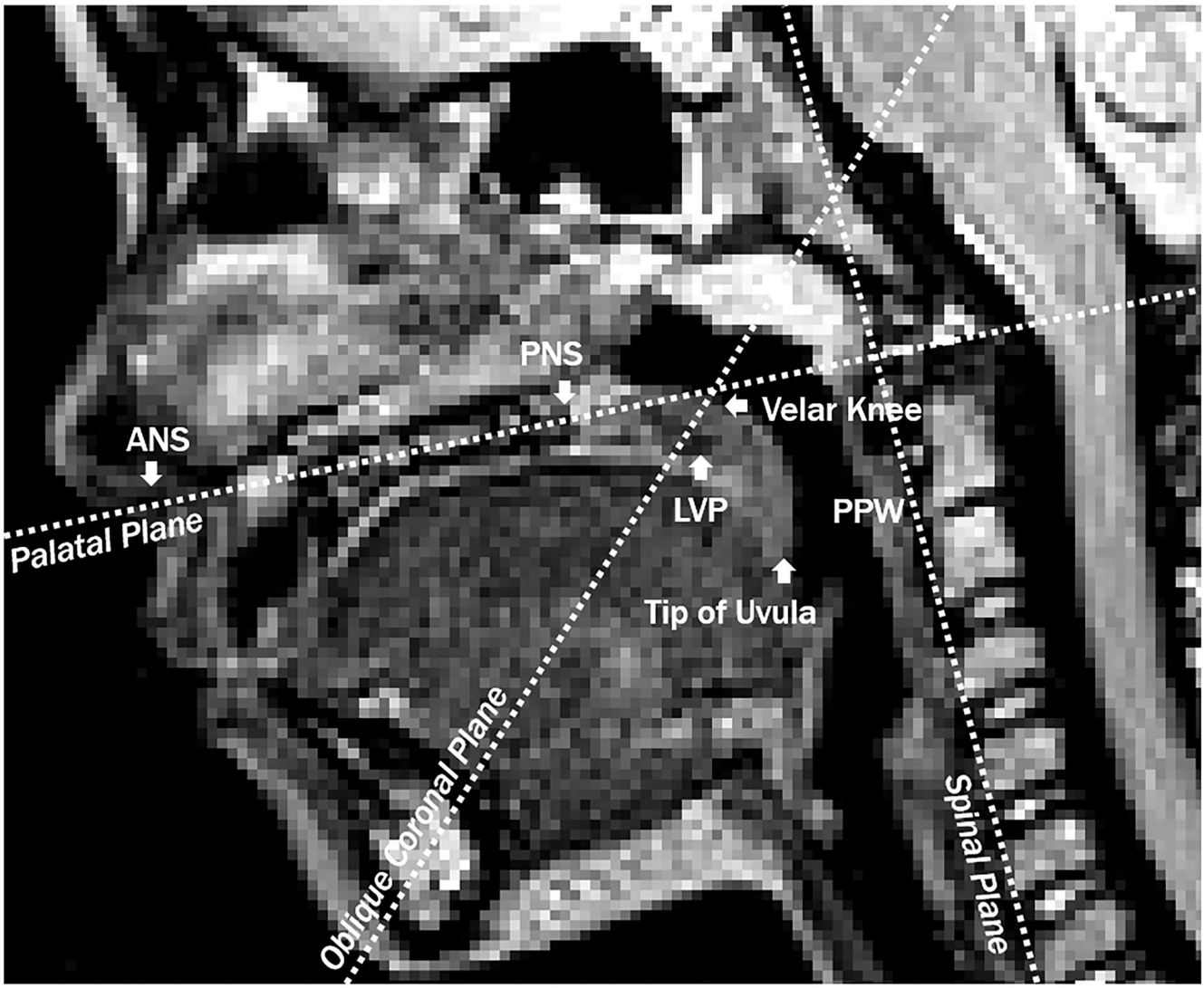

Figure 1.

Measures of the velopharynx were obtained from the midsagittal imaging plane using the anatomical landmarks and planes labeled below. ANS = anterior nasal spine, PNS = posterior nasal spine, LVP = levator veli palatini muscle, PPW = posterior pharyngeal wall.

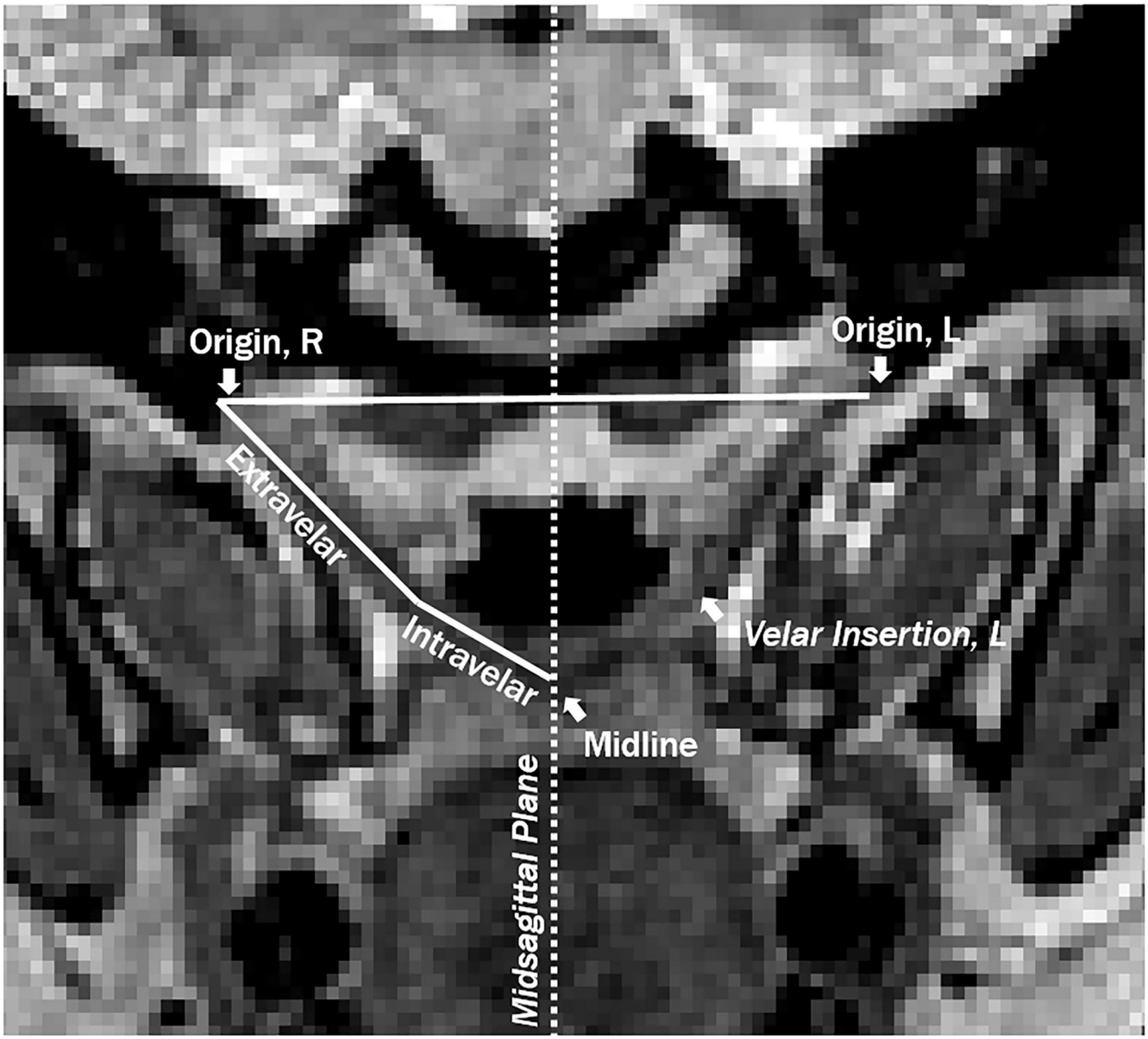

Figure 2.

Measures of the levator veli palatini (LVP) muscle were obtained from an oblique coronal image plane coursing parallel to the muscle using the anatomical landmarks and plane labeled below.

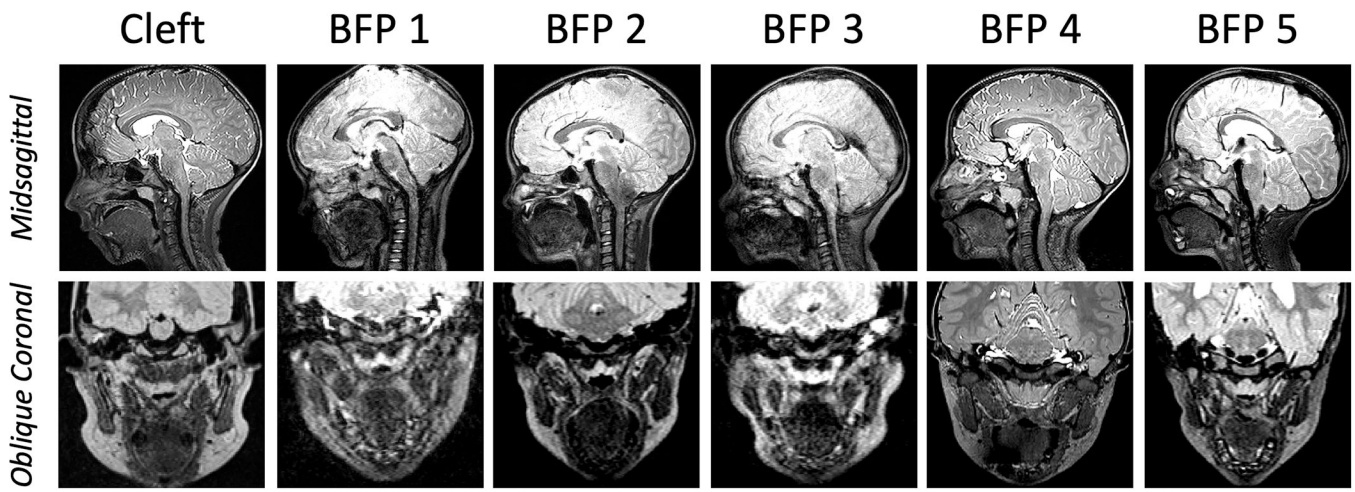

Figure 3.

Midsagittal (top row) and corresponding oblique coronal (bottom row) images of a single participant in the traditional cleft group and all 5 participants in the cleft with pedicled buccal fat pad (BFP) flap group.

Table 1.

Results of Kruskal-Wallis H test and pairwise comparisons for VP variables. Pertinent pairwise comparisons are displayed.

Variable	Median	H-test		Pairwise		
		χ^2	*P*-value	Mean Ranks		*P*-value
ANS-PNS	BFP: 34.77	3.551	.169			
	Cleft: 37.47					
	Non: 40.26					
Velar Length	BFP: 28.60	6.320	**.042** *	BFP: 9.20	Non: 10.80	1.000
	Cleft: 19.10			Cleft: 4.00	BFP: 9.20	.198
	Non: 27.70			Non: 10.80	Cleft: 4.00	**.049** *
PNS-PPW	BFP: 14.87	1.230	.533			
	Cleft: 17.67					
	Non: 16.92					
VP Ratio	BFP: 2.05	3.780	.151			
	Cleft: 1.40					
	Non: 1.93					
Effective Velar Length	BFP: 17.37	6.080	**.048** *	BFP: 12.00	Non: 6.40	.143
	Cleft: 11.51			Cleft: 6.60	BFP: 12.00	.071
	Non: 11.82			Non: 6.40	Cleft: 6.60	1.000
Velar Knee-PPW	BFP: 4.21	3.660	.160			
	Cleft: 8.16					
	Non: 9.00					
Effective VP Ratio	BFP: 1.20	6.140	**.046** *	BFP: 11.60	Non: 7.80	.537
	Cleft: .61			Cleft: 4.60	BFP: 11.60	**.040** *
	Non: .70			Non: 7.80	Cleft: 4.60	.774
Velar Thickness (midline)	BFP: 9.44	4.020	.134			
	Cleft: 6.99					
	Non: 9.13					
Sagittal Angle	BFP: 59.4	.636	.728			
	Cleft: 57.00					
	Non: 63.10					

* indicates significant result, $p < .05$; All values are in mm with the exception of angle (°), and ratio (no units) variables.

Table 2.

Results of Kruskal-Wallis H test and pairwise comparisons for levator veli palatini (LVP) muscle variables. Pertinent pairwise comparisons are displayed.

Variable	Median	H-test		Pairwise		
		χ^2	*P*-value	Mean Ranks		*P*-value
Velar Insertion Distance	BFP: 20.44	1.280	.527			
	Cleft: 20.27					
	Non: 19.06					
Origin-Origin Distance	BFP: 44.67	7.020	**.030** *	BFP: 3.80	Non: 11.00	**.033** *
	Cleft: 49.70			Cleft: 9.20	BFP: 3.80	.169
	Non: 55.15			Non: 11.00	Cleft: 9.20	1.000
Angle of Origin	BFP: 55.9	4.348	.114			
	Cleft: 54.8					
	Non: 48.6					
LVP Length	BFP: 33.48	7.760	**.021** *	BFP: 3.60	Non: 9.20	1.000
	Cleft: 38.89			Cleft: 11.20	BFP: 3.60	**.022** *
	Non: 36.73			Non: 9.20	Cleft: 11.20	.143
Extravelar Length	BFP: 23.28	9.420	**.009** *	BFP: 3.00	Non: 10.80	**.033** *
	Cleft: 25.64			Cleft: 10.20	BFP: 3.00	**.017** *
	Non: 26.55			Non: 10.80	Cleft: 10.20	1.000
Intravelar Length	BFP: 10.48	4.940	.085			
	Cleft: 12.24					
	Non: 10.29					
LVP Thickness (velar insertion)	BFP: 3.53	2.180	.336			
	Cleft: 3.86					
	Non: 3.01					
LVP Thickness (midline)	BFP: 3.38	1.340	.512			
	Cleft: 3.57					
	Non: 3.77					

* indicates significant result, $p < .05$; All values are in mm with the exception of angle (°), and ratio (no units) variables.